Effect of B₄C on the Microstructure and Mechanical Properties of As-Cast TiB+TiC/TC4 Composites

Jiheng Wang · Xianglong Guo · Lv Xiao · Liqiang Wang · Weijie Lu · Baohui Li · Zhongquan Li · Di Zhang

Abstract   Different additions of B₄C were introduced into TC4 to alter the microstructure and mechanical properties. The morphologies of reinforcements are related to the solidification paths. The refinement of lamellar spacing λ is based on the precipitation pattern of β-phases. Microhardness, compression elastic modulus (E_c), and elastic modulus of the matrix (E_m) appear non-linear relationships with B₄C additions. Due to the refinement of lamellar spacing with Hall–Petch-type relationships, and the solution strengthening of C on the $\alpha + \beta$ matrix, the effect of reinforcements on the mechanical properties will be more efficient when the additions of B₄C are no more than 0.19 wt%. When the additions of B₄C are more than 0.19 wt%, the efficiency will decrease.

KEY WORDS: Titanium matrix composites; Lamellar spacing λ; Microstructure; TiC; TiB; Nanoindentation

1 Introduction

In the past decades, titanium matrix composites (TMCs) which were reinforced with ceramic particles have received a considerable attention because of their potential for the improvement in properties and service temperature. Due to the better interface of reinforcements/matrix and the lower preparation cost, traditional ingot metallurgy plus self-propagation high-temperature synthesis reaction between titanium and B₄C have become a popular way to produce TiB and TiC reinforced TMCs [1, 2]. However, the machining properties of these composites are inferior because of the distribution of the reinforcements with high hardness in the soft matrix. The difficulty in machining a workpiece with complex configuration restricts the application and development of the TMCs. Therefore, investment casting will be a good way to shape TMCs [3].

Among titanium alloys, TC4 is one of the most commonly used casting alloys and there is a continuous drive to improve its mechanical properties through alloy designs. In this study, different additions of B₄C were introduced into TC4 to improve its mechanical properties [4, 5]. Because of the additions of B₄C, the solidification paths of the TMCs are different from TC4, and greatly change the microstructure and mechanical properties of the TMCs. The effect of the additions of B₄C on the microstructure and mechanical properties of TMCs is important to the casting. Therefore, in this study, the effort was carried out to study the influence of B₄C on the microstructure and mechanical properties of as-cast TiB+TiC/TC4 composites.

J. Wang · X. Guo · L. Wang · W. Lu (✉) · D. Zhang
State Key Laboratory of Metal Matrix Composite, Shanghai Jiaotong University, Shanghai 200240, China
e-mail: luweijie@sjtu.edu.cn

J. Wang
School of Material Science and Engineering, Jiangsu University of Science and Technology, Zhenjiang 212003, China

L. Xiao · B. Li · Z. Li
Shanghai Research Institute of Spaceflight Precision Machinery, Shanghai 201600, China

Table 1 Compositions of TiB+TiC/TC4 composites

Sample	TiB+TiC (TiB:TiC $\approx$ 4:1) (vol%)	Al–47.5V alloy (wt%)	Al (wt%)	B_4C (wt%)	Ti
TC4	0	8.43	1.57	0	Bal.
TMC1	0.5	8.39	1.56	0.10	Bal.
TMC2	1	8.34	1.55	0.19	Bal.
TMC3	5	8.00	1.49	0.97	Bal.
TMC4	10	7.56	1.41	1.93	Bal.
TMC5	20	7.00	1.25	3.86	Bal.
TMC6	30	5.84	1.09	5.76	Bal.

2 Experimental

Six different compositions of TiB+TiC/TC4 composites were manufactured and examined. Stoichiometric amounts of sponge titanium, Al, Al–V alloy with 47.5 wt% V and B_4C powder were blended and melted in non-consumable vacuum arc-melting furnace. The ingots were button shape with a diameter of 35 mm and a thickness of 20 mm. The weight percentage of reactants and theoretical volume percentage of reinforcements are listed in Table 1. To achieve the chemical homogeneity of the TMCs, the ingots were melted at least three times. In order to study the effects of reinforcements, TC4 was also produced by the same method.

All samples were wire cut from the central position of cast ingots. The microstructures of the as-cast samples were characterized by Philips XL30W/TMP scanning electron microscope (SEM). The microhardness of TiB+TiC/TC4 composites was measured using a Vickers pyramidal indenter with a fixed load (2 N) and loading time (10 s) on a HVS-10 digital microhardness apparatus. The compression tests were conducted on Sans5105 electromechanical universal testing machine. The compression test specimens were cylinders with diameter of 10 mm and height of 15 mm. The elastic modulus of the matrix was tested by the CSM nanoindentation testing system with the maximum load of 100 mN and the loading rate of 200 mN/s.

3 Results and Discussion

3.1 Microstructures

The micrographs of TiB+TiC/TC4 composites incorporating with the Ti–B–C ternary phase diagram are shown in Fig. 1. The distribution, shape, and scale of TiB and TiC reinforcements are changed with increasing additions of B_4C. The reinforcements with short fiber or needle shapes

are identified as TiB phases, whereas the reinforcements with dendritic or equiaxed shape are identified as TiC phases [6–9]. When the B_4C less than 0.97 wt% is added, the reinforcements are mainly precipitated along the prior β-grain boundaries, as shown in Fig. 1b–d, which indicates that the reinforcements are not potential sites for the heterogeneous nucleation of β-grains. In Fig. 1e, the reinforcements distribute uniformly in the matrix. In Fig. 1f, the primary TiB phases exhibit a great growth. In Fig. 1g, the primary TiC phases with dendritic shape disperse in the matrix. The TiB phases with big fiber shape are also observed in the matrix.

All these differences of reinforcements can be accounted for the solidification paths of the alloys according to the Ti–B–C ternary phase diagram [10]. Since the process temperature of non-consumable vacuum arc-melting furnace used in this experiment is much higher than 2,000 °C, TiB and TiC reinforcements are completely melt in the liquid titanium in course of the fabrication according to the projection of liquidus surfaces in Ti–B–C ternary phase diagram [10]. During the cooling processing, TiB and TiC reinforcements precipitate from liquid titanium alloy and grow up. The solidification paths of TMC1, TMC2, and TMC3 are illustrated in Fig. 2a. In TMC1, TMC2, and TMC3, the β-Ti phase is a primary phase. As a consequence, the reinforcements are precipitated after the primary β-Ti phase and are pushed aside along the grain boundaries. However, in TMC3, because of the closeness to the ternary eutectic reaction, the amount of primary β-Ti is relatively small, the large scale TiB_m whiskers are precipitated in the matrix with β-Ti_m, and ternary eutectic of (β-Ti+TiB+TiC)$_e$ is also observed in the matrix. The solidification path of TMC4 is shown in Fig. 2b; the TiB phase is a primary phase, and TiB_p phase grows up and is longer than TiB phase in TMC3. Because of the closeness to the ternary eutectic reaction, TiB_p cannot grow too large, and then the following precipitations of (β-Ti+TiB)$_m$ will take place soon. With the weight of B_4C addition increasing, the composition of TiB+TiC/TC4 composites is far away from ternary eutectic reaction. As a consequence, there are some large primary phases of reinforcements observed in the TMCs. The solidification path of TMC5 is shown in Fig. 2c; the TiB_p is the primary phase, and TiB_p whiskers grow up with width of almost 40 μm. With the temperature decrease, the binary eutectics of (TiC+TiB)$_m$ are precipitated in the molten metal liquid. Finally, the ternary eutectics of (β-Ti+TiB+TiC)$_e$ are solidified from the liquid, and all the liquid change into a solid. The solidification path of TMC6 is shown in Fig. 2d. TiC_p is the primary phase with dendritic shape. The binary eutectics of (TiC+TiB)$_m$ are precipitated after primary phase TiC_p. Therefore, coarsening TiB whiskers are also observed in the matrix. As is the case with TMC5, the last
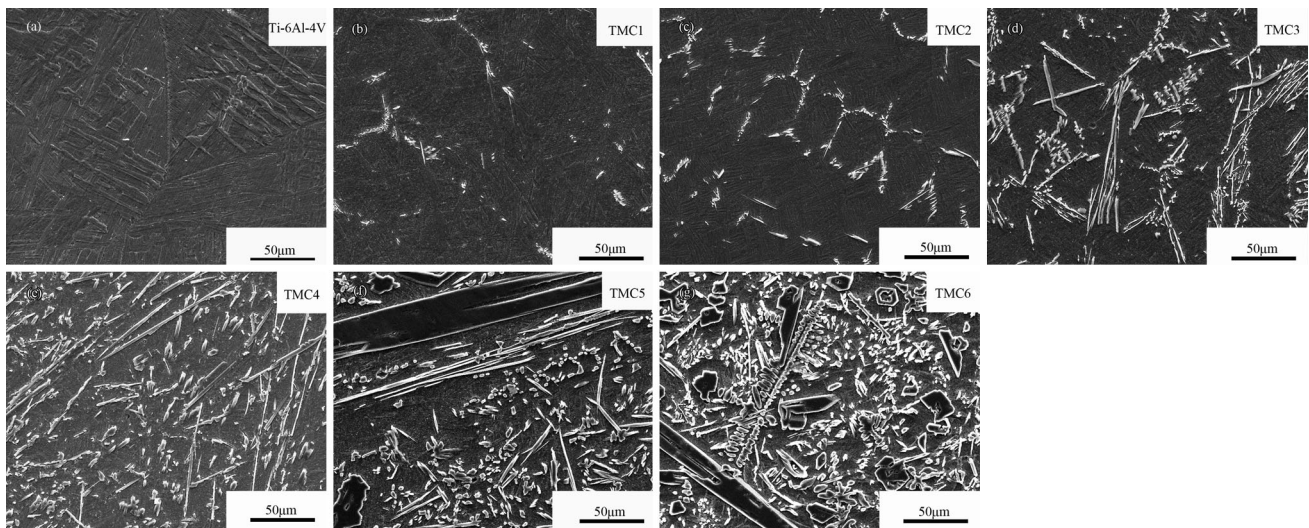
Fig. 1 SEM morphologies of TiB+TiC/TC4 composites with different additions of B$_4$C: **a** Ti–6Al–4V; **b** TMC1; **c** TMC2; **d** TMC3; **e** TMC4; **f** TMC5; **g** TMC6
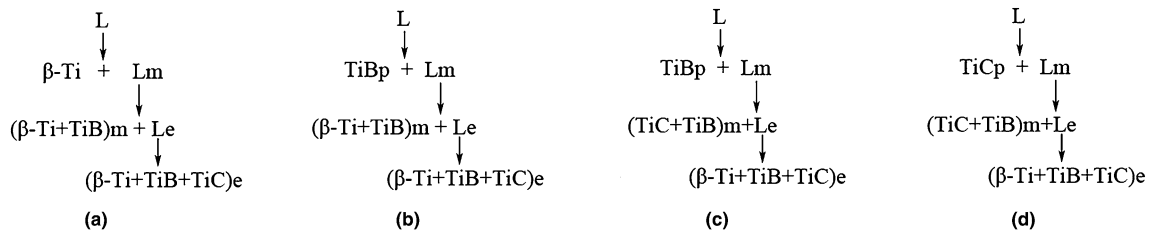

Fig. 2 Solidification paths of TiB+TiC/TC4 composites (where the subscripts p, m, and e denote the primary phase, binary eutectic, and ternary eutectic point, respectively): **a** TMC1, TMC2, TMC3; **b** TMC4; **c** TMC5; **d** TMC6

precipitated one is also ternary eutectic of (β-Ti+TiB+TiC)$_e$.

The lamellar spacing λ is measured by the space between two closing center lines of α lamellas. The variations of λ (obtained over 50 lamellar spacing per each sample) are affected by the contents of B$_4$C, as shown in Fig. 3. The prior β-grain size and lamellar spacing λ of TC4 alloy are markedly fined with the appearance of TiB and TiC phases. The addition of 0.10 wt% B$_4$C refines the λ size from 4.8 to 1.47 μm with a decrease of approximate 70%. The precipitations of reinforcements are located along the prior β-grain boundaries, which indicated that the reinforcements are not potential sites for the heterogeneous nucleation of β-grain, and the refinement in the size of the primary β-titanium grains occurred due to constitutional under-cooling during solidification [11]. When the weight of B$_4$C additions increases to 0.97 wt%, λ decreases from 1.47 to 1.36 μm. This phenomenon is similar to the results reported by Sen et al. [12]. When additions of B$_4$C increase to 1.93 wt%, the refinements will take place again and λ decreases from 1.36 to 0.97 μm. After that, further additions of B$_4$C will not refine the λ. According to the solidification path of TMCs, the refinement of λ is based on the
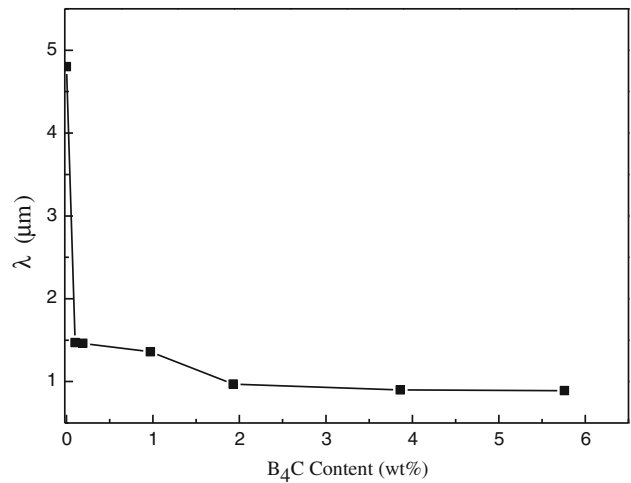

Fig. 3 Variation of lath thickness of TiB+TiC/TC4 composites with different additions of B$_4$C

precipitation pattern of β-phases. If most of β-phases are the primary phases, the λ is refined by B$_4$C and decrease to about 30%, as shown in TMC1, TMC2, and TMC3. If most
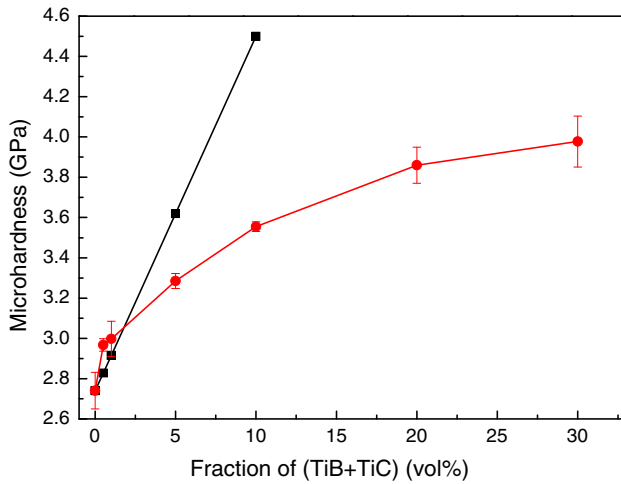
Fig. 4 Variation of microhardness of TiB+TiC/TC4 composites with different volume fractions of TiB+TiC

of β-phases are precipitated from ternary eutectic reaction, the λ is refined by B_4C and decrease to about 20%, as shown in TMC4, TMC5, and TMC6.

3.2 Microhardness

The variation of microhardness of TiB+TiC/TC4 composites is plotted in Fig. 4. Additions of B_4C will increase the microhardness of TC4. The increasing tendency of microhardness is nonlinear with the volume of the reinforcements, which is also affected by the micrographs of TiB+TiC/TC4 composites. Due to relatively large imprints produced by loads, the possible predominant influence of either soft titanium matrix or hard reinforcements can be avoided. Moreover, the information with regard to average microhardness value of the composite can be obtained accurately [13]. The primary TiB and TiC phase with large scale have been avoided in TMC5 and TMC6. A theoretical model is proposed to describe the microhardness of composite [13]:

$$H_{TMCs} = H_p V_p + H_0 \left(1 - V_p\right),$$ (1)

where H_{TMCs} is the microhardness of TMCs, H_p is the microhardness of reinforcements, V_p is the volume fraction of reinforcements, and H_0 is the microhardness of alloy matrix. The following microhardness values of H have been reported for single reinforcement phases: $H_{TiC} = 32.5$ GPa [14], $H_{TiB} = 17.3$ GPa (the middle of range 13.8–20.8 GPa) [15]. Due to the existence of two different reinforcements, the mixture rule can be used:

$$H_p V_p = H_{TiC} V_{TiC} + H_{TiB} V_{TiB}.$$ (2)

Then, Eq. (1) can be modified as

$$H_{TMCs} = H_{TiC} V_{TiC} + H_{TiB} V_{TiB} + H_{TC4}(1 - V_{TiC} - V_{TiB}).$$ (3)

It can be seen from Fig. 4 that the experimental hardness of TMCs is little higher than which was estimated by Eq. (3) when the volume fraction of TiB+TiC is less than 1.0 vol% (0.19 wt% B_4C). This is the reason that the refinement of lamellar spacing λ with Hall–Petch-type relationship is not considered in the estimation formula [13], and the effect of solution strengthening of C on the hardness was also not taken into account which can increase the hardness [16, 17]. Assuming that these effects are independent, and therefore, the Eq. (3) can be modified as

$$H_{TMCs} = H_{TiC} V_{TiC} + H_{TiB} V_{TiB} + H_{TC4}(1 - V_{TiC} - V_{TiB}) + \Delta H_{refinement} + \Delta H_{solution},$$ (4)

where $\Delta H_{refinement}$ is the increment of microhardness due to grain refinement and $\Delta H_{solution}$ is the additional microhardness resulting from solid-solution strengthening. Using the Hall–Petch-type relationship, $\Delta H_{refinement}$ can be described as

$$\Delta H_{refinement} = \frac{k}{\sqrt{\lambda}},$$ (5)

where k is a material constant. $\Delta H_{solution}$ can be described as

$$\Delta H_{solution} = \eta \varepsilon_s^{3/2} c^{1/2},$$ (6)

where η *is* a material constant and ε_s is the interaction parameter which is related to the effects of elastic and atomic size mismatch. Substituting the Eqs. (5), (6) to (4), the microhardness for TMCs can be described as

$$H_{TMCs} = H_{TiC} V_{TiC} + H_{TiB} V_{TiB} + H_{TC4}(1 - V_{TiC} - V_{TiB}) + \frac{k}{\sqrt{\lambda}} + \eta \varepsilon_s^{3/2} c^{1/2}.$$ (7)

When the volume fraction of TiB+TiC is more than 5 vol% (0.97 wt% B_4C), the experimental values are less than those obtained from estimation. Because TMC4, TMC5, and TMC6 are per-eutectic structures, the preliminary structure is eutectic structures, and the large scale per-eutectic particles of TiB and TiC phases have been avoided in the test. Thus, H_{TMCs} is close to the microhardness of eutectic structures and the experimental values are less than those obtained from estimation.

3.3 Elastic Modulus

Figure 5 shows the compression test results. All samples did not crush under 1,150 MPa, as shown in Fig. 5a. The
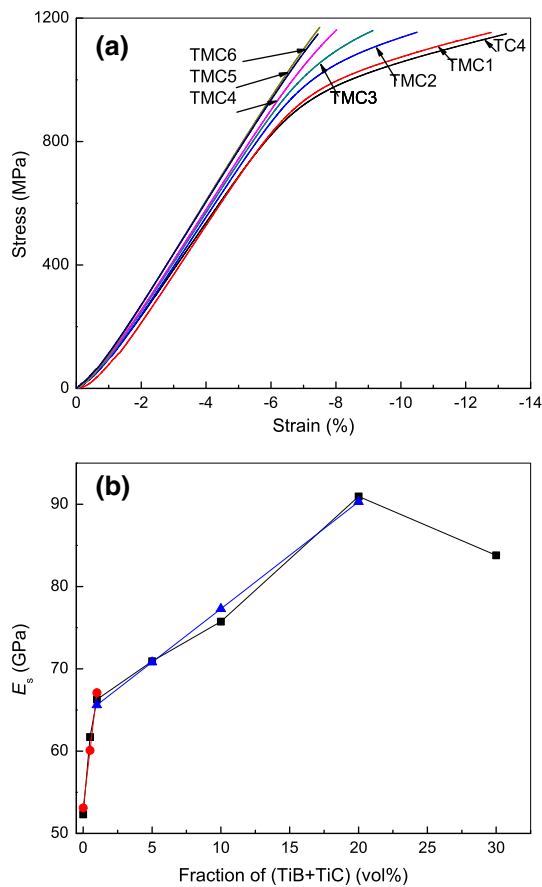
Fig. 5 The compression test results of TiB+TiC/TC4 composites: **a** the stress–strain curves of compression tests; **b** variation of E_c of TiB+TiC/TC4 composites with different volume fractions of TiB+TiC

Fig. 6 Variation of elastic modulus of TiB+TiC/TC4 composites matrix with different volume fractions of TiB+TiC

compressing elastic modulus (E_c) is obtained from the slopes of loading curves, as shown in Fig. 5b. It can be observed that B$_4$C additions lead to the increase of E_c and it has a similar tendency with the microhardness, as shown in Fig. 4, but there are two inflection points in the curve. A good linear scaling of E_c can be seen with volume fraction of TiB+TiC between 0 and 1 vol% (0–0.19 wt% B$_4$C), while a different linear scaling of E_c can be seen with volume fraction of TiB+TiC between 1 and 20 vol% (0.19–3.86 wt% B$_4$C). When the volume fraction of TiB+TiC is more than 20 vol% (3.86 wt% B$_4$C), the E_c drops.

When $V_{TiC+TiB} < 1$ vol%, the fitting linear equation can be written as

$$E_c = 53.1 + 1,400\,V_{TiC+TiB}, \tag{8}$$

when 1 vol% $< V_{TiC+TiB} < 20$ vol%, the fitting linear equation can be written as

$$E_c = 64.3 + 130\,V_{TiC+TiB}. \tag{9}$$

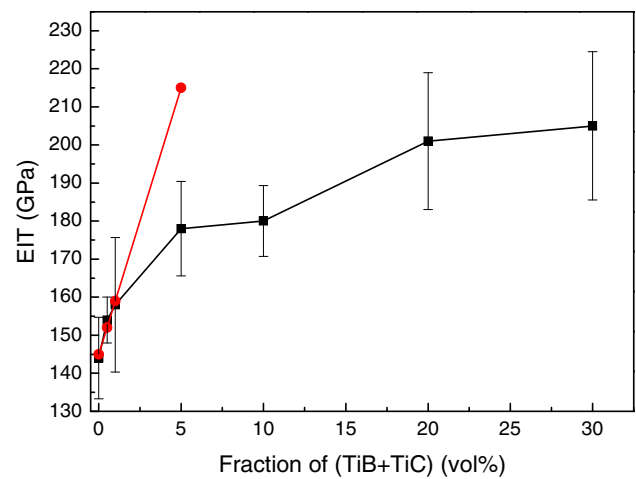This result can be explained through the microstructures of TiB+TiC/TC4 composites. When the addition of B$_4$C is no more than 0.19 wt%, the TiB or TiC reinforcements are settled on the grain boundary, and most of the β-phases are the primary phase and the eutectic structure is of little amount. The E_c increases dramatically not only because of the formation of TiC and TiB, but also the solution strengthening of C in the α + β matrix. With the addition of B$_4$C increasing, the matrix is saturated and the solution strengthening effect can not contribute the enhancement of E_c any more. With TiB phase coarsing, the reinforcement efficiency of TiB phase in the overall system decreases, so the curve of E_c become smoothly. When the content of B$_4$C increases to 5.76 wt%, most TiC phases with dendritic shape are precipitated in the matrix, which makes the reinforcement efficiency of TiC phase in the overall system decreased. At the same time, because of the low mobility of liquid TMCs, shrinkage porosity even shrinkage cavity can be seen in the matrix and this makes the E_c of TMC6 lower than TMC5. Therefore, E_c decreases when the volume fraction of TiB+TiC is more than 20 vol%.

The elastic modulus of the matrix (E_m) measured by nanoindentation is shown in Fig. 6. The TiB and TiC phases have been avoided during the test. Due to relatively large imprints (about 15 μm) produced by loads and the relatively small lamellar spacing λ (about 0.9–4.8 μm) of α + β, the possible predominant influence of either α phase or β-phase can be avoided. Moreover, the information with regard to average elastic modulus of the α + β matrix can be obtained accurately.

When $V_{TiC+TiB} < 1$ vol%, the fitting linear equation is written as

$$E_m = 145 + 1,400\,V_{TiC+TiB}. \tag{10}$$

From Eqs. (8) and (10), the slope values of both E_c and E_m are 1,400, which represent that the increase of elastic modulus is based on the solution strengthening of C on the α + β matrix when addition of B$_4$C is less than 0.19 wt%.

The elastic modulus can be increased by the carbon dissolved in the titanium due to the solution strengthening effects which are related to the mass fraction in solution [18, 19]. When $V_{TiC+TiB}$ more than 1 vol%, the curve slope of E_c and E_m will decrease, i.e., the elastic modulus increases slowly. Therefore, the effect of reinforcements on the mechanical properties will be more apparent when the addition of B_4C is no more than 0.19 wt%. When the addition of B_4C is more than 0.19 wt%, the effect will decrease.

4 Conclusions

The addition of B_4C to TC4 modifies the solidification behavior of the alloy, and also alters its microstructure and mechanical properties.

(1) The morphologies of reinforcements are related to the solidification paths.
(2) The lamellar spacing λ is refined with the addition of B_4C, and the refinement of λ is based on the precipitation pattern of β-phases.
(3) Microhardness, compression elastic modulus, and elastic modulus of the matrix measured by nanoindentation appear a non-linear relationship with B_4C additions, which increase dramatically when the addition of B_4C is no more than 0.19 wt%. Due to the refinement of lamellar spacing i with Hall–Petch-type relationships, and the solution strengthening of C on the $\alpha + \beta$ matrix, the effect of reinforcements on the mechanical properties will be more apparent when the additions of B_4C are no more than 0.19 wt%. When the additions of B_4C are more than 0.19 wt%, the effect will decrease.

References

[1] S. Ranganath, M. Vijayakumar, J. Subrahmanyan, Mater. Sci. Eng. A **149**, 253 (1992)
[2] X. Zhang, W. Lü, D. Zhang, R. Wu, Y. Bian, P. Fang, Scr. Mater. **41**, 39 (1999)
[3] B.J. Choi, Y.J. Kim, Mater. Trans. **52**, 1926 (2011)
[4] J. Lu, J. Qin, W. Lu, D. Zhang, H. Hou, Z. Li, Mater. Sci. Eng. A **500**, 1 (2009)
[5] E. Yun, K. Lee, S. Lee, Surf. Coat. Technol. **184**, 74 (2004)
[6] W. Lu, D. Zhang, X. Zhang, S.L. Guo, R.J. Wu, Trans. Nonferrous Met. Soc. China **11**, 67 (2001)
[7] W. Lu, D. Zhang, X. Zhang, R. Wu, T. Sakata, H. Mori, J. Alloys Compd. **327**, 240 (2001)
[8] W. Lu, D. Zhang, X. Zhang, R. Wu, T. Sakata, H. Mori, J. Alloys Compd. **327**, 248 (2001)
[9] J. Zhu, A. Kamiya, T. Yamada, W. Shi, K. Naganuma, Mater. Sci. Eng. A **339**, 53 (2003)
[10] P. Villars, A. Prince, H. Okamoto, *Handbook of ternary alloy phase diagrams*, vol. 5 (ASM International, Materials Park, 1995)
[11] R. Srinivasan, S. Tamirisakandala, Scr. Mater. **63**, 1244 (2010)
[12] I. Sen, S. Tamirisakandala, D. Miracle, U. Ramamurty, Acta Mater. **55**, 4983 (2007)
[13] B. Mordyuk, M. Iefimov, G. Prokopenko, T. Golub, M. Danylenko, Surf. Coat. Technol. **204**, 1590 (2010)
[14] Y. Yang, H. Lu, C. Yu, J. Chen, J. Alloys Compd. **485**, 542 (2009)
[15] F.C. Wang, Z. Zhang, J. Luo, C.C. Huang, S.K. Lee, Compos. Sci. Technol. **69**, 2682 (2009)
[16] C. Schuh, T. Nieh, H. Iwasaki, Acta Mater. **51**, 431 (2003)
[17] A. Suzuki, N.D. Saddock, L. Riester, E. Lara-Curzio, J. Jones, T. Pollock, Metall. Mater. Trans. A **38**, 420 (2007)
[18] Ø. Ryen, B. Holmedal, O. Nijs, E. Nes, E. Sjölander, H.-E. Ekström, Metall. Mater. Trans. A **37**, 1999 (2006)
[19] Y. Mishima, S. Ochiai, N. Hamao, M. Yodogawa, T. Suzuki, Jpn Inst. Met. Trans. **27**, 656 (1986)